

Ni-doped $\text{CoFe}_2\text{O}_4/\text{C}$ nanoparticles as efficient catalysts for ORR in alkaline media.

By: Mphoma Matseke
Supervisors: Dr H. Zheng

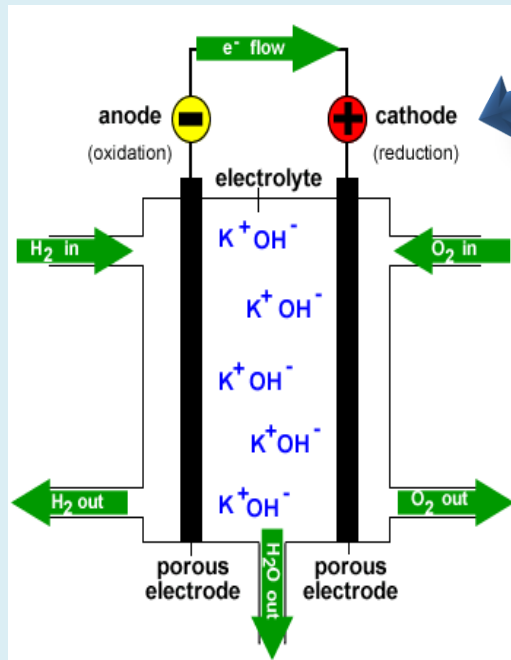
12 August 2019

Contents

- 1 Introduction
- 2 Aims and objectives
- 3 Methodology
- 4 Results
- 5 Conclusions
- 6 References
- 7 Acknowledgements

Introduction

Oxygen reduction reaction



Reaction pathways in alkaline media

1. $O_2 + 2H_2O + 4e^- \rightarrow 4OH^-$
($4e^-$ reduction pathway)
1. $O_2 + H_2O + 2e^- \rightarrow HO_2^- + OH^-$
 $H_2O + HO_2^- + 2e^- \rightarrow 3OH^-$
($2e^-$ reduction pathway)

Introduction Cont...

Spinel ferrites

- Spinel ferrites are compounds with general formula of $A[B_2]O_4$.

Where A = Divalent metal ions (Fe^{2+} , Co^{2+} , Ni^{2+} , etc.)

B = Trivalent metal ions (Fe^{3+})

- They have cubic close packings of O^{2-} ions.
- They are made up of two types of sites: Tetrahedral sites (**A-sites**)
Octahedral sites (**B-sites**)

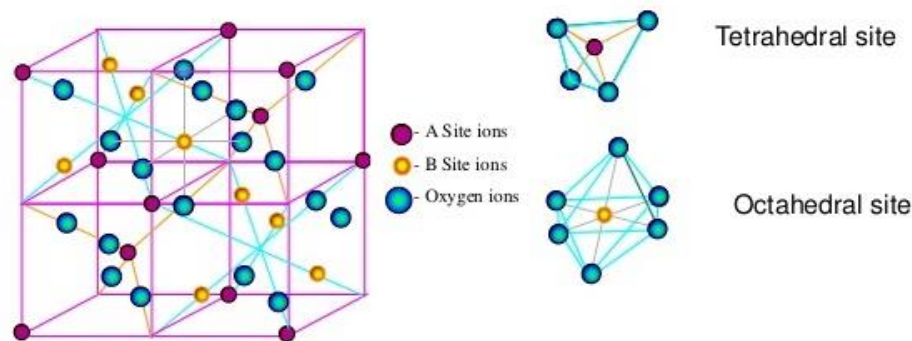


Figure 1. Typical spinel structure.

Introduction Cont...

Classification of spinels

- Normal spinel structure : $\delta = 1$; $M^{2+}[Fe^{3+}]O_4^{2-}$; e.g. $ZnFe_2O_4$
- Inverse spinel structure : $\delta = 0$; $Fe^{3+}[M^{2+}Fe^{3+}]O_4^{2-}$; e.g. $CoFe_2O_4$ $NiFe_2O_4$
- Mixed spinel structure : $0 < \delta < 1$; $M_{1-\delta}^{2+}Fe_{\delta}^{3+}[M_{\delta}^{2+}Fe_{2-\delta}^{3+}]O_4^{2-}$; e.g. $MnFe_2O_4$

Why spinel ferrites?

Because of their controllable composition, structural robustness, low cost, accessibility, ease and mode of synthesis, desirable activity and environmental friendliness.

Aims and Objectives

The main aim of this work was to synthesize carbon-supported $\text{Ni}_x\text{Co}_{1-x}\text{Fe}_2\text{O}_4$ nanoparticles with high catalytic activity for ORR in alkaline media.

The objectives were thus to:

- Synthesize $\text{Ni}_x\text{Co}_{1-x}\text{Fe}_2\text{O}_4$ ($x = 0, 0.25, 0.5, 0.75$ and 1) electrocatalysts through the hydrothermal method;
- Employ the XRD, FTIR, HRTEM, EDX and SAED techniques to characterize the synthesized catalysts;
- Investigate the electrochemical performances of the synthesized catalysts for ORR in O_2 -saturated 0.1 M KOH electrolyte through the use of CV and LSV the techniques.

Methodology

Step 1



Sonication

10 min



Step 2

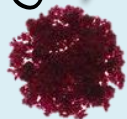


HO

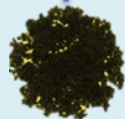
OH

DI +
(CH₂OH)₂

CoCl₂·6H₂O



FeCl₃



NiCl₂·6H₂O



- Stir for 15 min.
- Add the CB solution and stir for 15 min.
- Add urea and stir for additional 15 min.
- Transfer the mixture into a Teflon cup.
- Subjection to hydrothermal reaction at 150 °C for 17 h.

XRD Measurements

$$d = \frac{\lambda}{2\sin\theta} \dots\dots\dots(1)$$

$$a = d\sqrt{(h)^2 + (k)^2 + (l)^2} \dots\dots\dots(2)$$

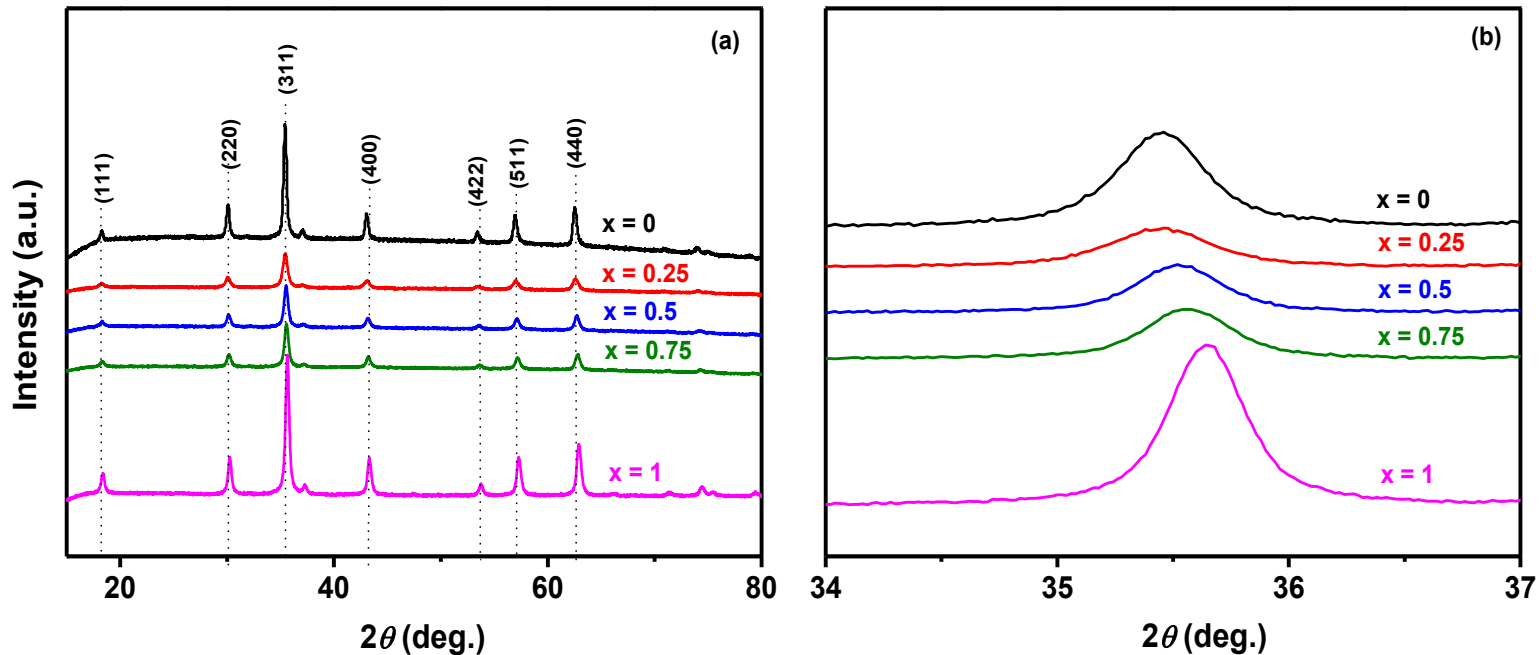


Figure 2. (a) (X-ray diffraction patterns of $\text{Ni}_x\text{Co}_{1-x}\text{Fe}_2\text{O}_4/\text{C}$ ($x = 0, 0.25, 0.5, 0.75$ and 1), (b) the partially enlarged XRD patterns indicating the (311) peaks.

XRD Measurements Cont...

Table 1 XRD data of $\text{Ni}_x\text{Co}_{1-x}\text{Fe}_2\text{O}_4/\text{C}$ ($x = 0, 0.1, 0.25, 0.5, 0.75$ and 1) calculated from the (311) diffraction peak.

Sample (x)	Crystallite size D (nm)	2θ (deg.)	d -spacing (nm)	Lattice parameter a (Å)
0	28.56	35.50	0.252 ± 0.0009	8.387 ± 0.0007
0.25	17.09	35.43	0.253 ± 0.0004	8.404 ± 0.0003
0.5	20.57	35.49	0.252 ± 0.0009	8.387 ± 0.0007
0.75	20.58	35.53	0.252 ± 0.0007	8.381 ± 0.0001
1	23.99	35.62	0.252 ± 0.0000	8.357 ± 0.0009

FTIR Analysis

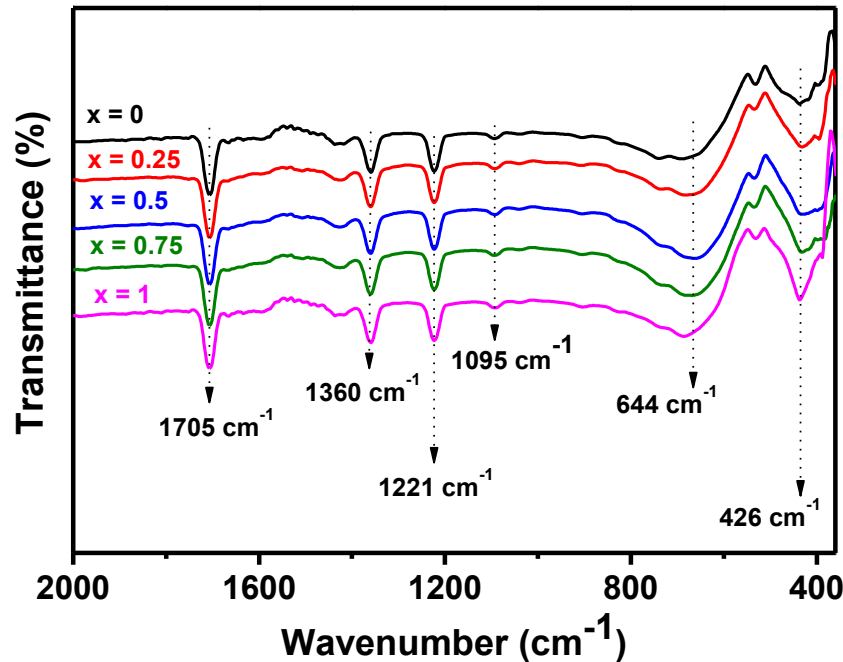


Table 2 Assignment of FTIR spectra and variation of higher (ν_1) and lower (ν_2) bands with an increase in the Ni^{2+} concentration.

Sample (x)	ν_1 (cm^{-1})	ν_2 (cm^{-1})
0	644.22	426.27
0.25	638.44	432.05
0.5	640.37	430.12
0.75	663.51	433.84
1	671.22	437.84

Figure 3. FTIR spectra of $\text{Ni}_x\text{Co}_{1-x}\text{Fe}_2\text{O}_4/\text{C}$ ($x = 0, 0.25, 0.5, 0.75$ and 1) samples.

TEM and SAED Analysis

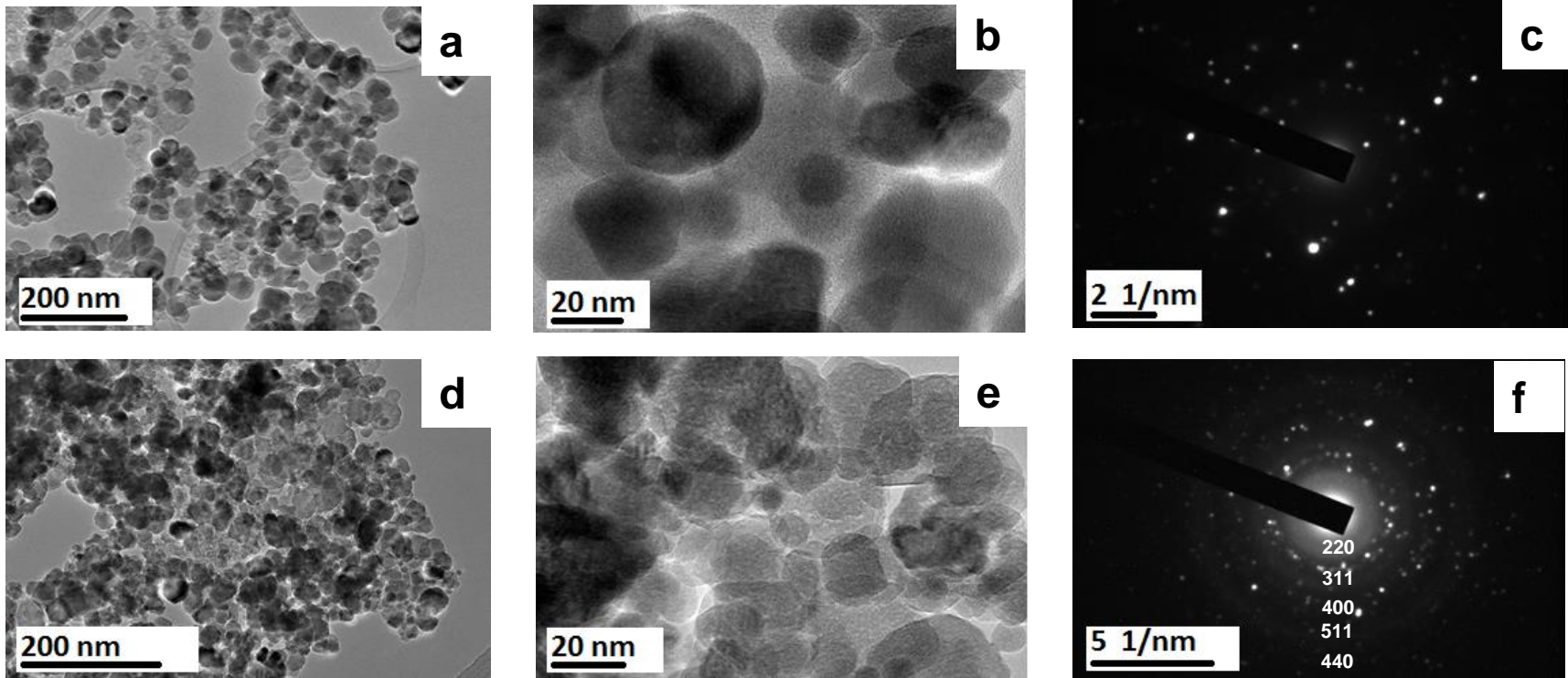


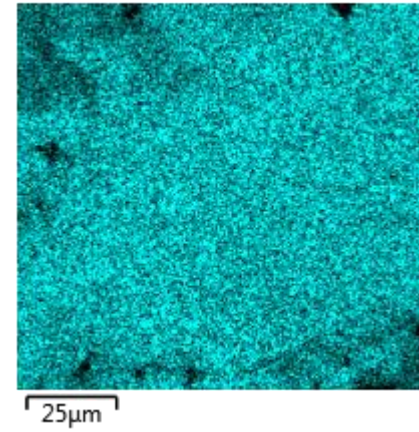
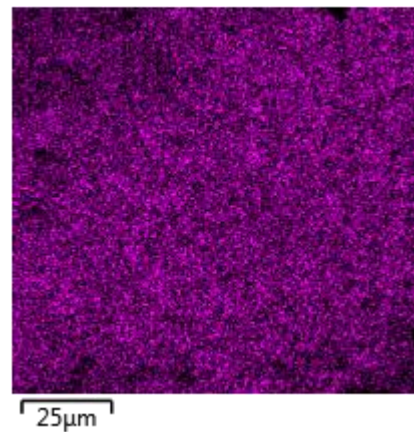
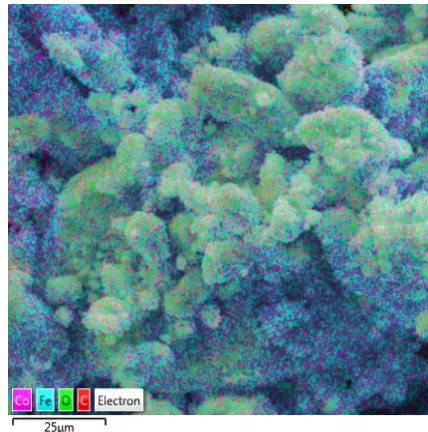
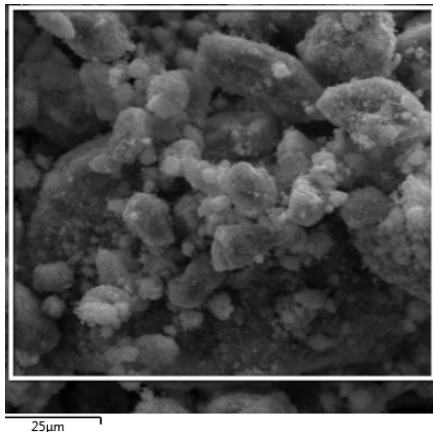
Figure 4. (a, b) TEM images of CoFe₂O₄/C. (d, e) TEM images of Ni_{0.75}Co_{0.25}Fe₂O₄/C. (c, f) SAED patterns of CoFe₂O₄/C (c) and Ni_{0.75}Co_{0.25}Fe₂O₄/C (f).

Elemental mapping and EDX Analysis

$\text{CoFe}_2\text{O}_4/\text{C}$

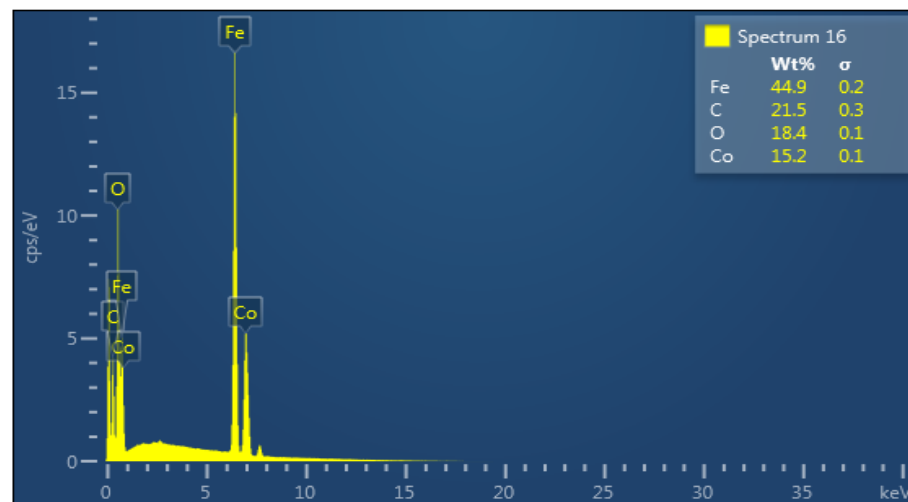
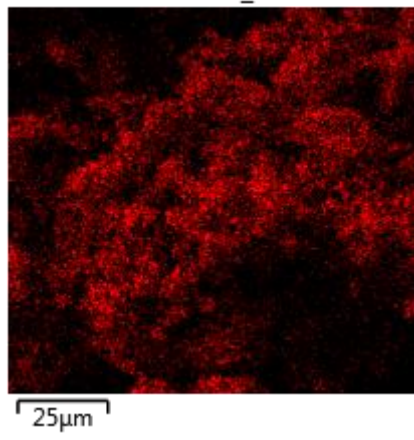
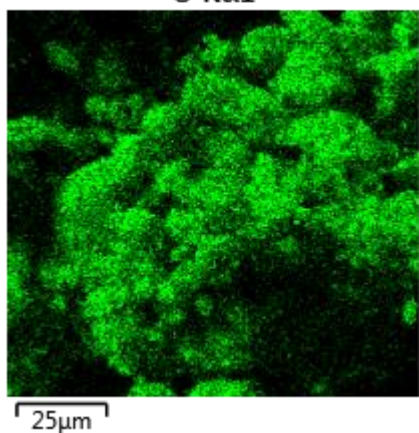
Co K α 1

Fe K α 1

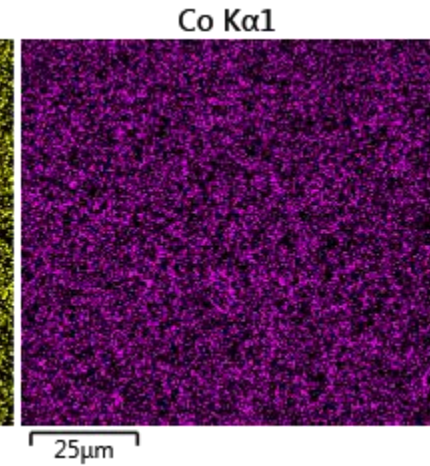
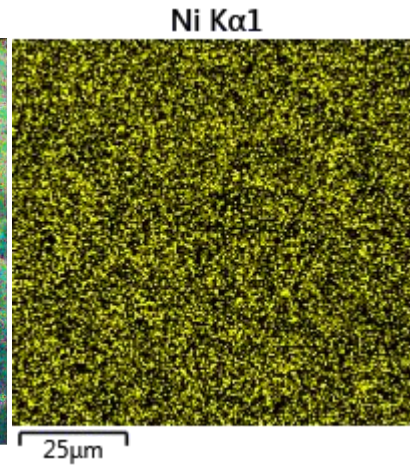
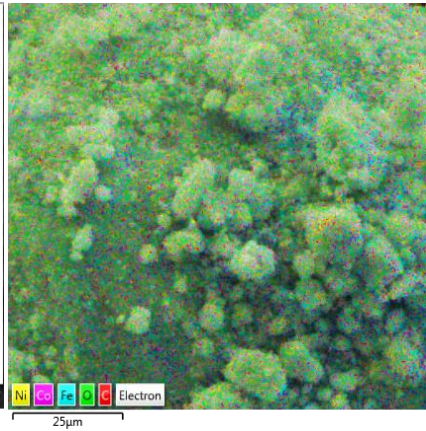
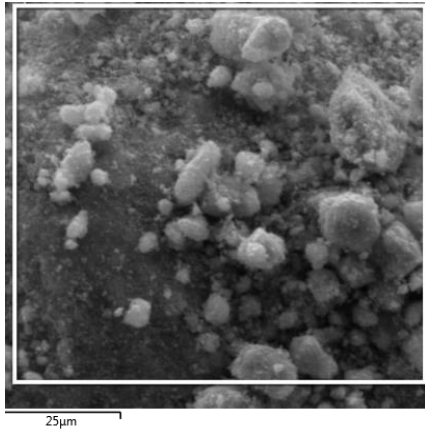


O K α 1

C K α 1_2



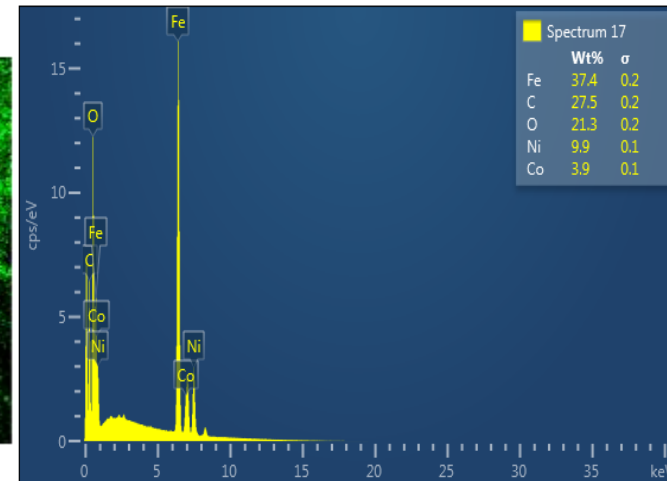
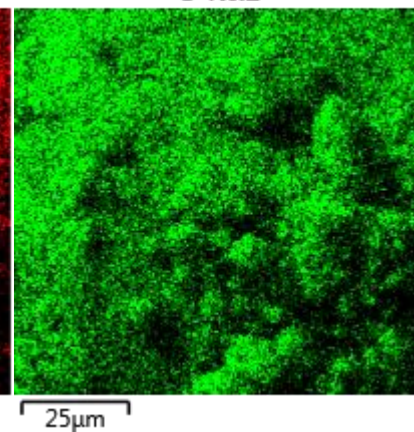
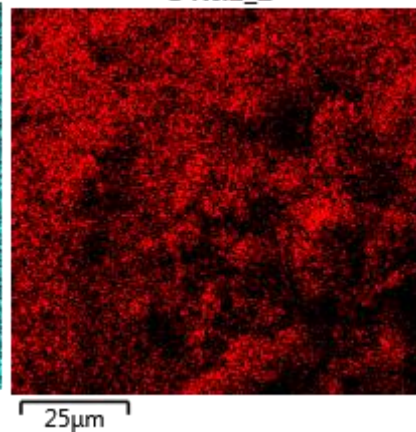
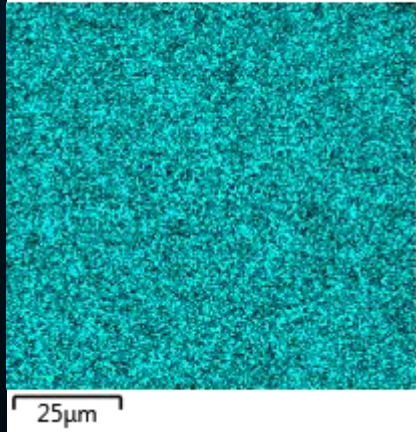
Elemental mapping and EDX Analysis Cont...



Fe K α 1

C K α 1_2

O K α 1



Electrochemical measurements Cont...

Linear sweep voltammetry

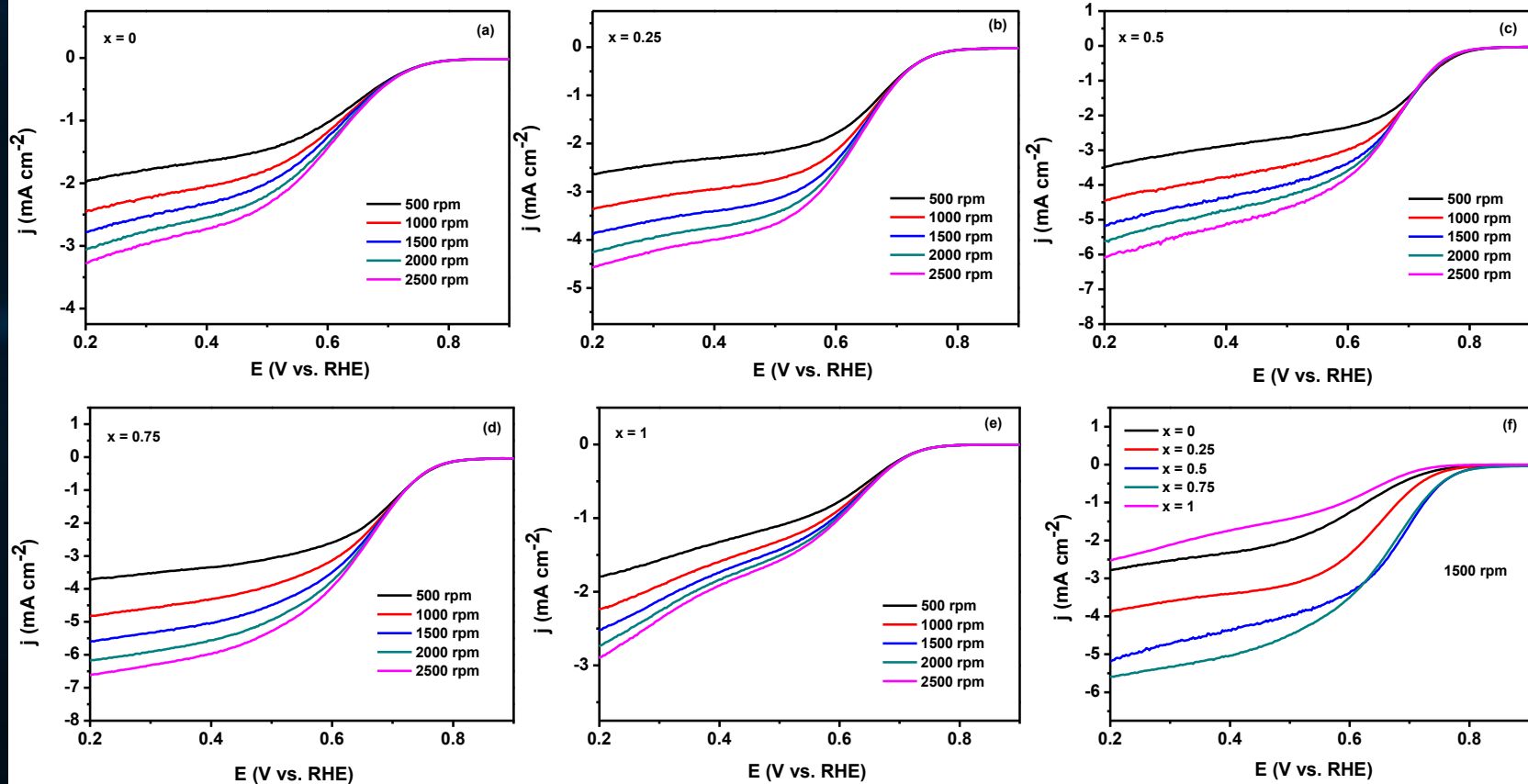


Figure 7. (a-e) LVS curves of $\text{Ni}_x\text{Co}_{1-x}\text{Fe}_2\text{O}_4/\text{C}$ catalysts. (f) Comparison of the LSV curves at 1500 rpm.

Electrochemical measurements

Cyclic Voltammetry

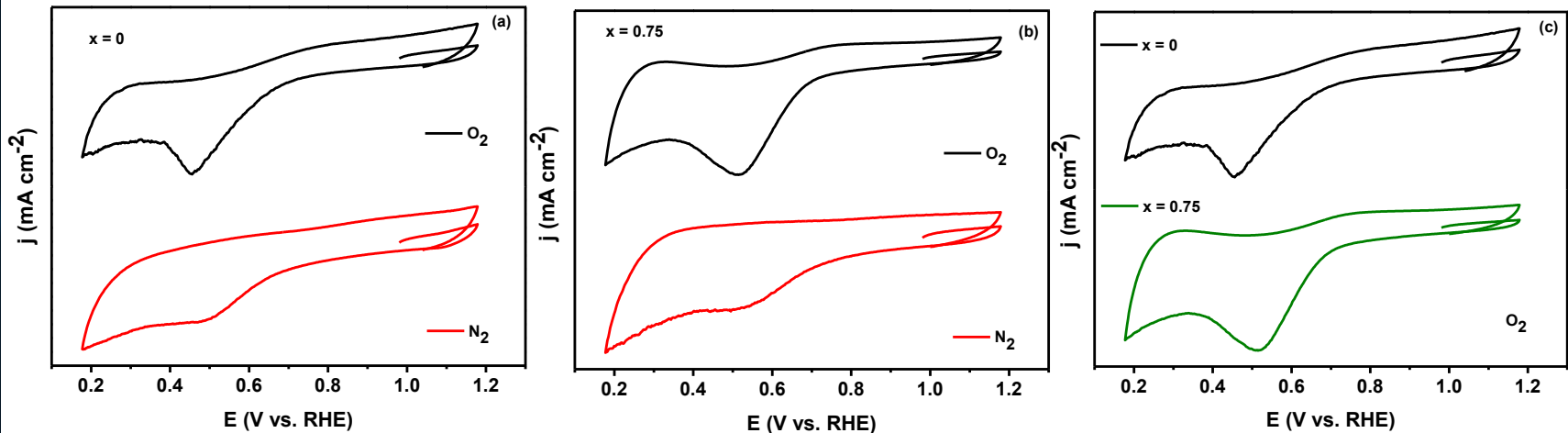


Figure 8. (a, b) CVs for $Ni_xCo_{1-x}Fe_2O_4/C$ ($x = 0$ and 0.75) in O_2 - and N_2 -saturated 0.1 M KOH solution and a scan rate of 50 mV/s. (c) Comparison of CVs for $Ni_xCo_{1-x}Fe_2O_4/C$ ($x = 0$ and 0.75) in O_2 -saturated solution.

Electrochemical measurements Cont...

Koutecky-Levich (K-L) plots Analysis

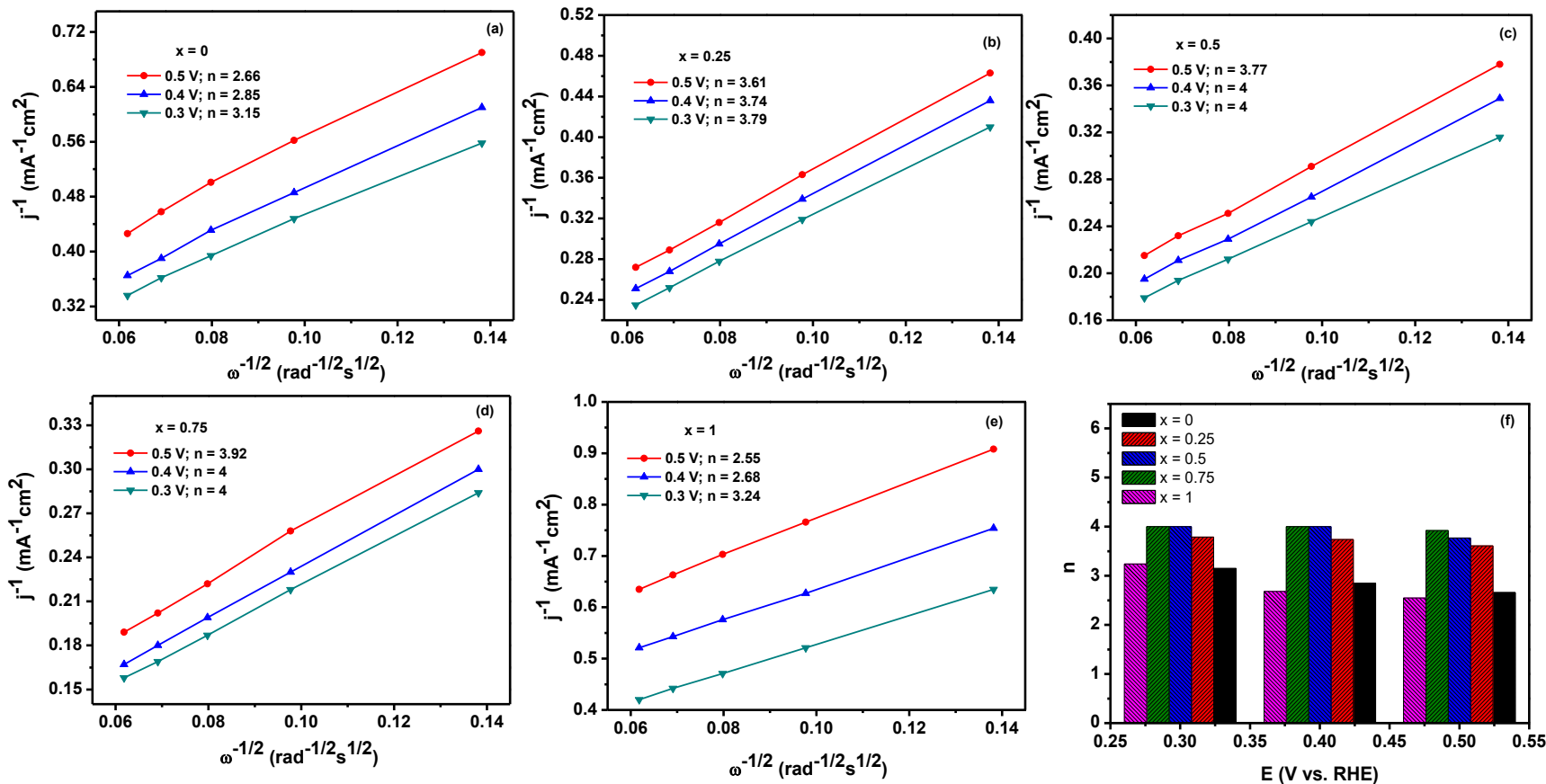


Figure 9. (a-e) K-L plots of $\text{Ni}_x\text{Co}_{1-x}\text{Fe}_2\text{O}_4/\text{C}$ catalysts. (f) Calculated n -values based on RDE data.

Electrochemical measurements Cont...

Tafel plot Analysis

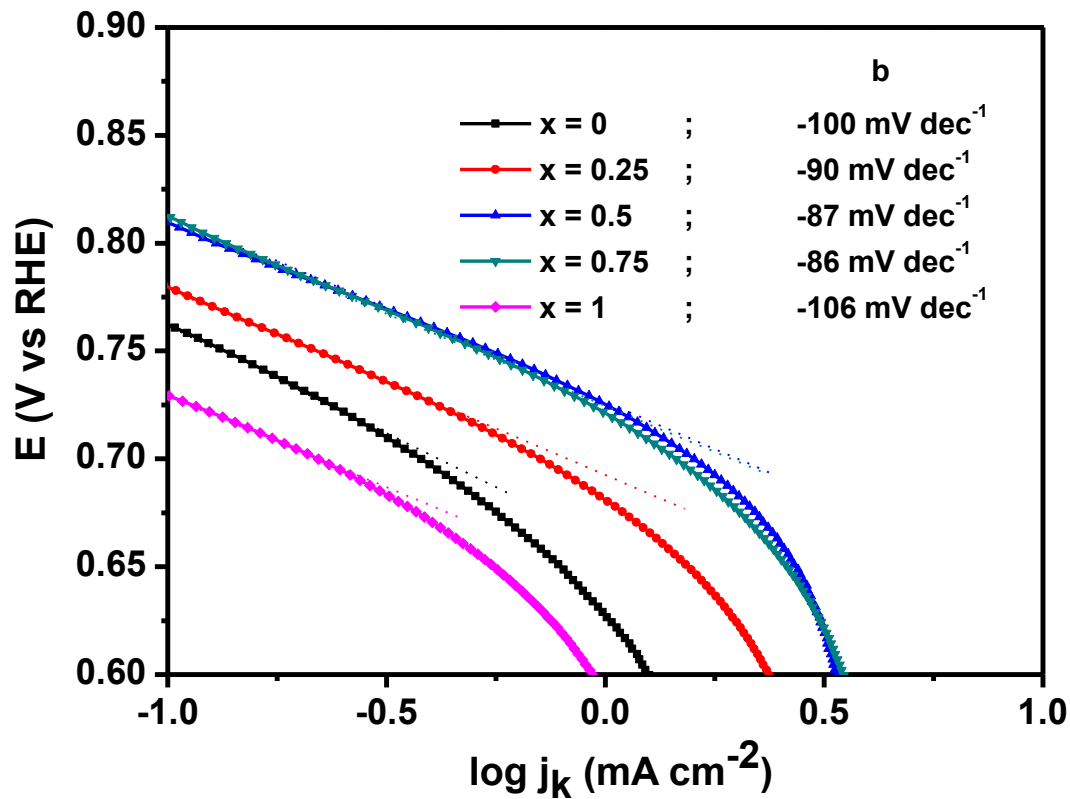


Figure 10. Tafel plots of $\text{Ni}_x\text{Co}_{1-x}\text{Fe}_2\text{O}_4/\text{C}$ catalysts at 1500 rpm.

Conclusions

- All the $\text{Ni}_x\text{Co}_{1-x}\text{Fe}_2\text{O}_4/\text{C}$ ($x = 0, 0.25, 0.5, 0.75$ and 1) catalysts were successfully synthesized through the hydrothermal method;
- The samples are single-phase spinel compounds with the XRD crystallite sizes of 28.56, 17.09, 20.57, 20.58 and 23.99 nm for $x = 0, 0.25, 0.5, 0.75$ and 1 , respectively.
- Partially doping $\text{CoFe}_2\text{O}_4/\text{C}$ with Ni causes a reduction in the lattice parameter (a).
- Among the $\text{Ni}_x\text{Co}_{1-x}\text{Fe}_2\text{O}_4/\text{C}$ ($x = 0, 0.25, 0.5, 0.75$ and 1) catalysts, the $x = 0.75$ exhibited the best ORR activity. The catalytic activity increases in the order: $x = 1 < 0 < 0.25 < 0.5 < 0.75$.
- Ni-doped $\text{CoFe}_2\text{O}_4/\text{C}$ nanoparticles synthesized through the hydrothermal method at a low temperature could be potential cathode materials for ORR in alkaline fuel cells.

References

1. Bhujun, B.; Tan, M.T.; Shanmugam, A.S. Study of mixed ternary transition metal ferrites as potential electrodes for supercapacitor applications. *Results Phys.* **2017**, *7*, 345-353.
2. He, H-Y. Structural and magnetic property of $\text{Co}_{1-x}\text{Ni}_x\text{Fe}_2\text{O}_4$ nanoparticles synthesized by hydrothermal method. *Int. J. Appl. Ceram. Technol.* **2014**, *11*, 626-636.
3. Wang, Y.; Liu, Q.; Zhang, L.; Hu, T.; Liu, W.; Liu, N.; Du, F.; Li, Q.; Wang, Y. One-pot synthesis of $\text{Ag-CoFe}_2\text{O}_4/\text{C}$ as efficient catalyst for oxygen reduction in alkaline media. *Int. J. Hydrog. Energy* **2016**, *41*, 22547-22553.
4. Xu, Y.; Bian, W.; Wu, J.; Tian, J-H.; Yang, R. Preparation and electrocatalytic activity of 3D hierarchical porous spinel CoFe_2O_4 hollow nanospheres as efficient catalyst for oxygen reduction reaction and oxygen evolution reaction. *Electrochim. Acta* **2015**, *151*, 276-283.
5. Omelyanchik, A.; Singh, G.; Volochaev, M.; Sokolov, A.; Rodionova, V.; Peddis, D. Tunable magnetic properties of Ni-doped CoFe_2O_4 nanoparticles prepared by the sol-gel citrate self-combustion method. *J. Magn. Magn. Mater.* **2019**, *476*, 387-391.
6. Torkian, S.; Ghasemi, A.; Razavi, R.S. Cation distribution and magnetic analysis of wideband microwave absorptive $\text{Co}_x\text{Ni}_{1-x}\text{Fe}_2\text{O}_4$ ferrites. *Ceram. Int.* **2017**, *43*, 6987-6995.
7. Dang, Z-M.; Wang, L.; Zhang, L-P. Surface functionalization of multiwalled carbon nanotube with trifluorophenyl. *J. Nanomater.* **2006**, Article ID 83583, 1-5.

References Cont...

8. Rana, S.; Philip, J.; Raj. Micelle based synthesis of cobalt ferrite nanoparticles and its characterization using Fourier Transform Infrared Transmission Spectrometry and Thermogravimetry. *Mater. Chem. Phys.* **2010**, 124, 264-269.
9. Wang, L.; Meng, H.; Shen, P.K.; Bianchini, C.; Vizza, F.; Wei, Z. In situ FTIR spectroelectrochemical study on the mechanism of ethylene glycol electrocatalytic oxidation at a Pd electrode. *Phys. Chem. Chem. Phys.* **2011**, 13, 2667–2673.
10. Boobalan, T.; Suriyanarayanan, N.; Pavithradevi, S. Structural, magnetic and dielectric properties of nanocrystalline cobalt ferrite by wet hydroxyl chemical route. *Mat. Sci. Semicon. Proc.* **2013**, 16, 1695-1700.
11. Habibi, M.H.; Parhizkar, H.J. FTIR and UV-vis diffuse reflectance spectroscopy studies of the wet chemical (WC) route synthesized nano-structure CoFe_2O_4 from CoCl_2 and FeCl_3 . *Spectrochim. Acta A* **2014**, 127, 102-106.
12. Adeela, N.; Maaz, K.; Khan, U.; Karim, S.; Nisar, A.; Ahmad, M.; Ali, G.; Han, X.F.; Duan, J.L.; Liu, J.; Influence of manganese substitution on structural and magnetic properties of CoFe_2O_4 nanoparticles. *J. Alloys Compd.* **2015**, 639, 533, 540.
13. Ati, A.A.; Othaman, Z.; Samavati, A. Influence of cobalt on structural and magnetic properties of nickel ferrite nanoparticles. *J. Mol. Struct.* **2013**, 1052, 177-182.

Acknowledgements

- Supervisors: Dr H. Zheng and Prof K. Mallick

- National Research Foundation (NRF)



- Council for Scientific and Industrial Research (CSIR)



- University of Johannesburg



Thank You